Available online at www.scholarsresearchlibrary.com

Scholars Research Library

Der Pharmacia Lettre, 2015, 7 (5):211-219
(http://scholarsresearchlibrary.com/archive.html)

Der Pharmacia Lettre
Scholars Research Library
ISSN 0975-5071
USA CODEN: DPLEB4

A quantum-chemical and docking study of the inhibitory activity of a family of thienopyrimidine derivatives bearing a chromone moiety against mTOR Kinase

Juan S. Gómez-Jeria* and Javier Valdebenito-Gamboa

Quantum Pharmacology Unit, Department of Chemistry, Faculty of Sciences, University of Chile. Las Palmeras 3425, Santiago, Chile

---

ABSTRACT

We present the results of docking and quantum-chemical studies of the relationships between the electronic/molecular structure and the inhibitory activity against the mTOR kinase by a group of recently synthesized thienopyrimidine derivatives bearing a chromone moiety. The electronic structure, including full geometry optimization, was obtained at the DFT B3LYP/6-31G(d,p) level. All molecules were also docked to a simplified model of mTOR kinase. Good results relating electronic structure and inhibitory percentage against mTOR kinase at a concentration of 10μM in vitro were obtained and the corresponding pharmacophore is proposed. Docking results suggest that all molecules interact with the same site and that short-range interactions of the C-H…O kind predominate. The question of the relationships between QSAR and docking results is analyzed.

Keywords: mTOR kinase, thienopyrimidine, QSAR, PI3K/AKT/mTOR pathway, chromone, kinases.

INTRODUCTION

The PI3K/AKT/mTOR pathway is an intracellular signaling pathway important in the regulation of the cell cycle (see Fig. 1 and [1, 2]). It is directly associated to cellular cancer, longevity, proliferation and quiescence. The PI3K pathway, in addition to its pro-proliferative and anti-apoptotic effects on tumor cells, is known to contribute to DNA-damage repair (DDR). Once activated, the PI3K/Akt/mTOR pathway can be propagated to a variety of substrates, including mTOR, a primary regulator of protein translation. The finding of PI3K/AKT/mTOR alterations and their roles in tumorigenesis, and its critical role in cell growth and survival, has made one of the preferred targets for the development of new molecules with potential for developing effective anticancer treatment. mTOR is a serine/threonine protein kinase that regulates aging, cell growth, cell proliferation, cell motility, cell survival, growth, immunity, memory, metabolism, protein synthesis, synaptic plasticity and transcription [3-58]. Abnormal mTOR activation leads to enhanced survival signaling in acute myeloid leukemia cells. mTOR belongs to the phosphatidylinositol 3-kinase-related kinase protein family. mTOR is the catalytic subunit of two distinct complexes called mTOR complex 1 (mTORC1) and mTORC2. The active site mTOR inhibitors represent a promising new approach to target the PI3K/AKT/mTOR pathway. Several molecules targeting different elements of this pathway have been synthesized and tested [8, 32, 59-105].

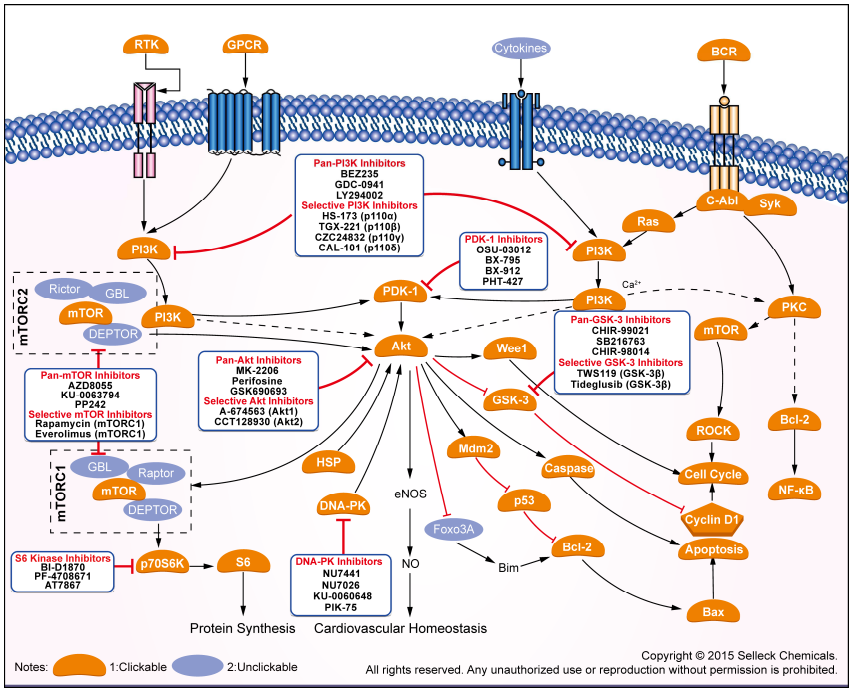

Figure 1. The PI3K/Akt/mTOR pathway (with permission of Selleckchem.com)

Here we present the results of docking and Density Functional Theory studies of the relationships between the electronic/molecular structure and the inhibitory activity against the mTOR kinase by a family of recently synthesized and tested thienopyrimidine derivatives bearing a chromone moiety [59]. We expect that these results will provide new information for a better understanding of mTOR inhibition.

METHODS, MODELS AND CALCULATIONS

A method to obtain physically-based structure-activity relationships is grounded on the following idea [106]. First, we suggest a model to explain a biological activity. Next, we apply one or more scientifically-based approximations and translate the assumptions of the model into one or more mathematical expressions. In our case, we started from the statistical-mechanical definition of the equilibrium constant, we have developed a formal method relating the electronic structure of drugs to their *in vitro* receptor affinity constant (K) [107-112]. The final result of this procedure is that, for the case of n molecules, we have the following system of n linear equations:

$$\log K_i = a + bM_{D_i} + c\log\left[\sigma_{D_i}/(ABC)^{1/2}\right] + \sum_j \left[e_j Q_j + f_j S_j^E + s_j S_j^N\right] +$$
$$+ \sum_j \sum_m \left[h_j(m) F_j(m) + x_j(m) S_j^E(m)\right] + \sum_j \sum_{m'} \left[r_j(m') F_j(m') + t_j(m') S_j^N(m')\right] +$$
$$+ \sum_j \left[g_j \mu_j + k_j \eta_j + o_j \omega_j + z_j \varsigma_j + w_j Q_j^{\max}\right] \quad (i=1,\ldots,n) \qquad (1)$$

where K_i is the affinity constant, M is the drug's mass, σ its symmetry number, ABC the product of the drug's moments of inertia about the three principal axes of rotation, Q_i is the net charge of atom i, S_i^E and S_i^N are, respectively, the total atomic electrophilic and nucleophilic superdelocalizabilities of Fukui et al., $F_{i,m}$ is the Fukui index (i.e., the electron population) of atom i in occupied (empty) MO (molecular orbital) m (m') [113]. $S_i^E(m)$ is the electrophilic superdelocalizability of atom i in occupied MO m, $S_i^E(m')$ is the nucleophilic superdelocalizability of atom i in empty MO m'. The last bracket on the right side of Eq. 1 contains local atomic reactivity indices obtained by an approximate reorganization of part of the remaining terms of the series expansion used in the model [114]. μ_j,

η_j, ω_j, ς_j and Q_j^{max} are the local atomic electronic chemical potential of atom j, the local atomic hardness of atom j, the local atomic electrophilicity of atom j, the local atomic softness of atom j and the maximal amount of electronic charge that atom j may accept. These new local atomic reactivity indices (LARIs) are expressed in eV like the global ones and not in eV·e as are the usual projected local reactivity indices coming from Density Functional Theory [114]. With this method, very good structure-activity relationships were obtained for a variety of drugs and receptors [115-128]. During year 2012 this method was extended to any biological activity with excellent results [129-149]

The selected molecules are shown in Fig. 2 and Table 1. The biological activity selected for this study is the inhibitory percentage against mTOR kinase at a concentration of 10μM *in vitro* (inhibitory % at 10μM). It is worth mentioning that this is first time that this kind of activity is analyzed with our method.

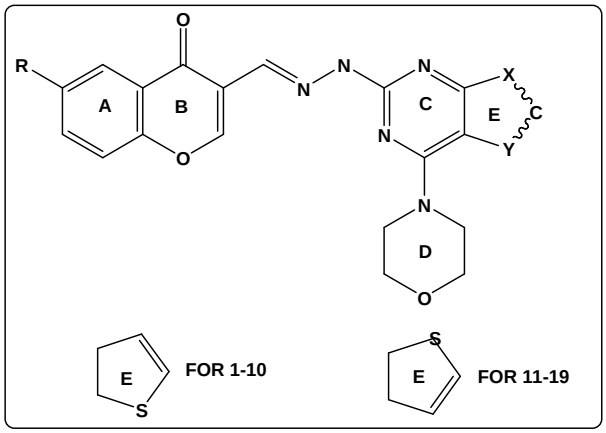

Figure 2. Molecules selected

Table 1. Molecules and biological activity

Mol.	R	log(inhibitory % at 10μM)
1	Cl	1.46
2	Br	1.62
3	Me	1.69
4	Et	1.51
5	*t*-Bu	1.40
6	OH	1.65
7	NO_2	1.73
8	Carboxyl	1.79
9	H	1.56
10	*i*-Pr	1.34
11	F	1.47
12	Cl	1.49
13	Br	1.49
14	Me	1.62
15	Et	1.43
16	*t*-Bu	1.54
17	OH	1.91
18	Carboxyl	1.99
19	H	1.63

We worked with the common skeleton hypothesis holding that the variation of the values of a group of reactivity indices belonging to a group of atoms common to all the molecules analyzed (the common skeleton) that accounts for almost all the variation of the biological activity. The effect of the substituents consists in modifying the electronic structure of this common skeleton and/or influencing the correct placement of the drug. The common skeleton is shown in Fig. 3 together with the atom numbering employed in the resulting equations.

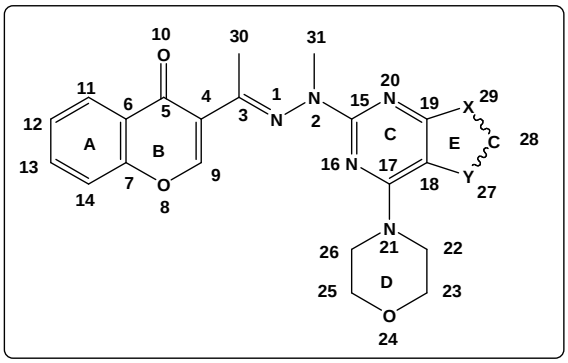

Figure 3. Common skeleton numbering

Molecular geometries were fully optimized at the B3LYP/6-31G(d,p) level of theory with the Gaussian package [150]. From the corrected Mulliken Population Analysis results [151] we obtained numerical values for all electronic local atomic reactivity indices (LARIS) appearing in Eq. 1. D-CENT-QSAR software was used [152]. Considering that the system of linear equations cannot be solved because the number of molecules is smaller than the number of unknown coefficients, a linear multiple regression analysis (LMRA) was carried out. The Statistica software was used [153]. For the docking study the Autodock Vina software was employed with a 40x30x40 box [154]. A truncated mTOR model was downloaded from the Protein Data Bank (PDB Id: 4JT6) and prepared for use with Autodock Vina after deleting a segment located very far from the binding site (Fig. 5).

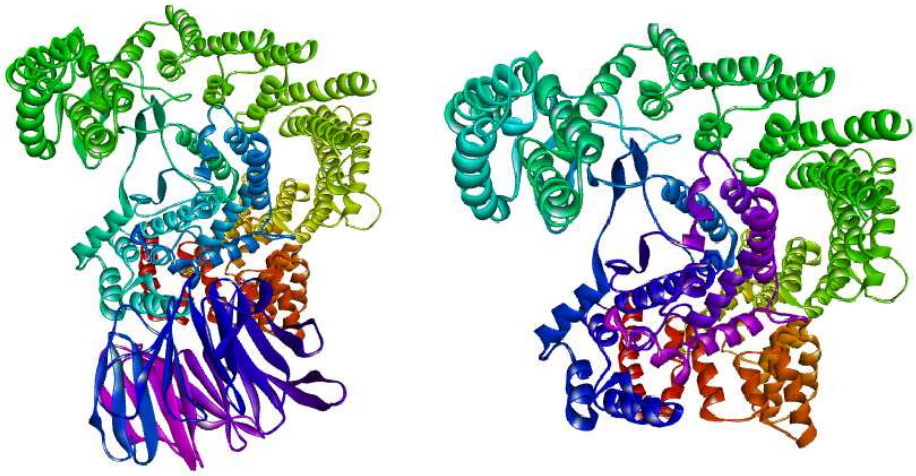

Figure 5. Original (left) and final (right) mTOR fragment

The lowest energy conformer of each study was selected for its analysis with Autodock Vina and Discovery Studio Visualizer [155].

RESULTS

Docking results

Figs. 5 to 9 show the docking results. Table 2 shows the definitions of the colors representing the interactions.

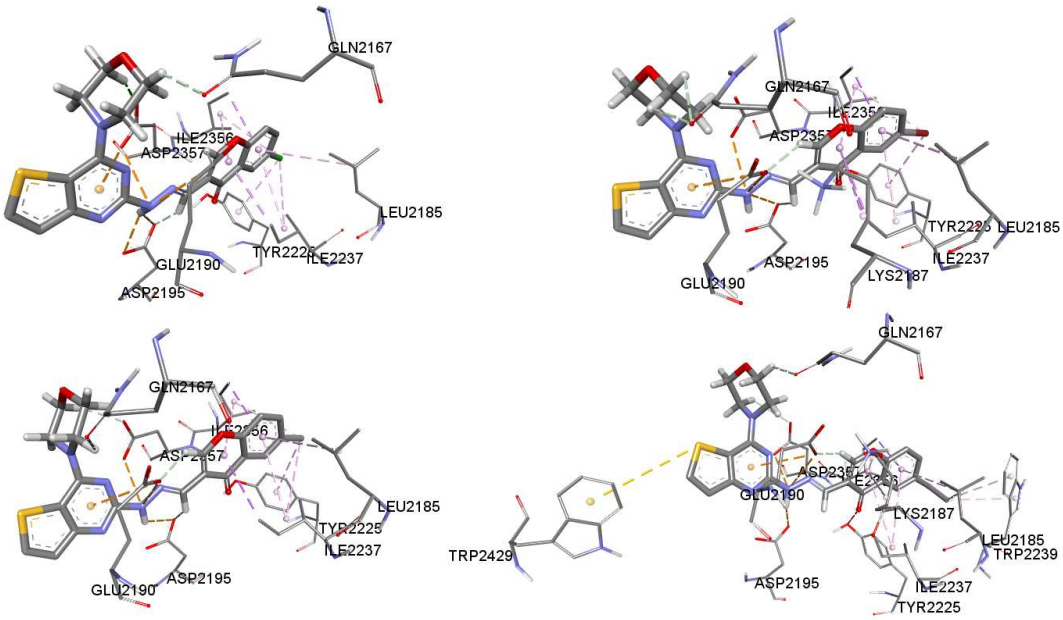

Figure 5. Docking results for molecules 1 (upper left), 2 (upper right), 3 (lower left) and 4 (lower right)

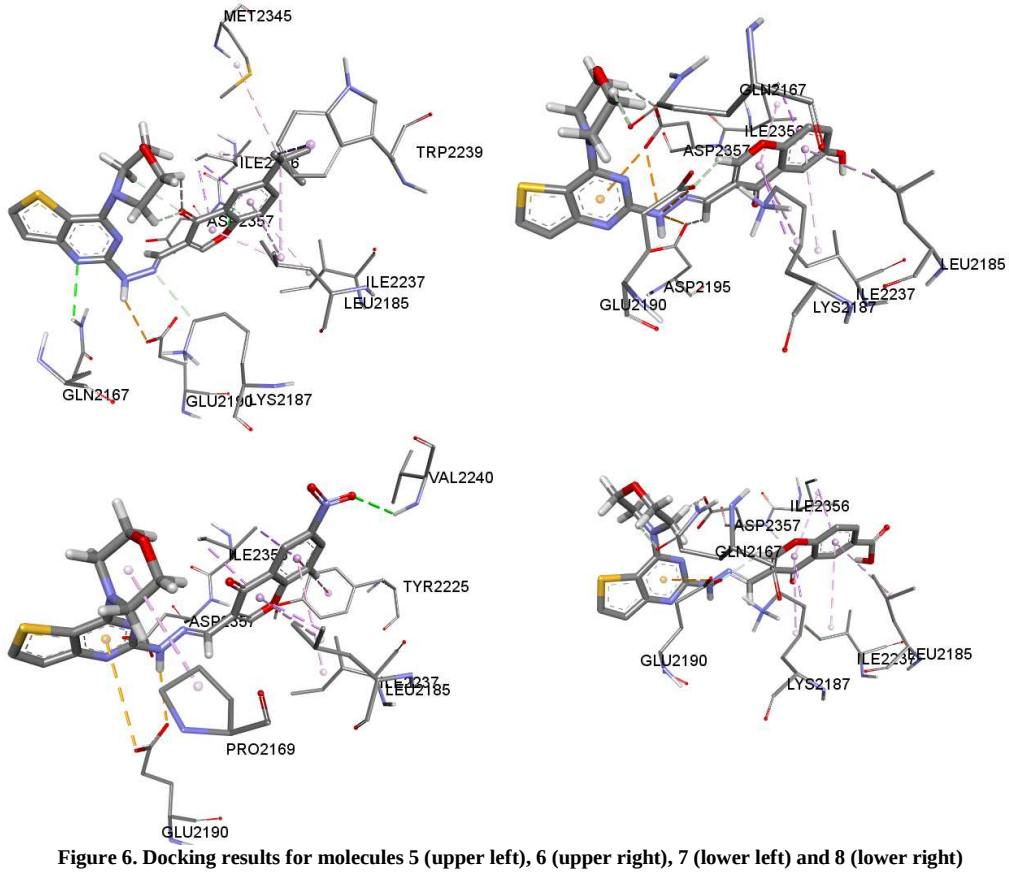

Figure 6. Docking results for molecules 5 (upper left), 6 (upper right), 7 (lower left) and 8 (lower right)

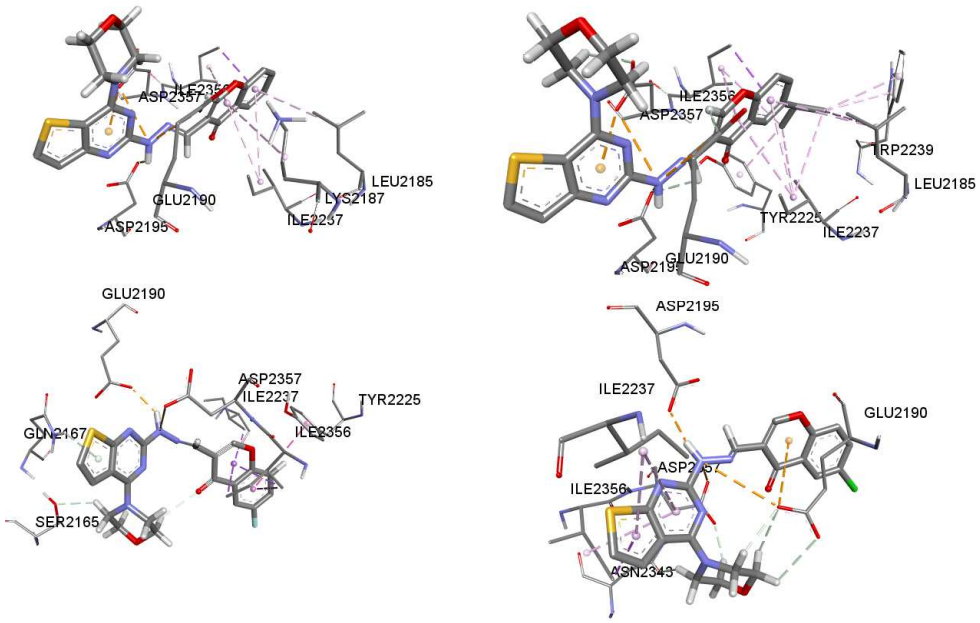

Figure 7. Docking results for molecules 9 (upper left), 10 (upper right), 11 (lower left) and 12 (lower right)

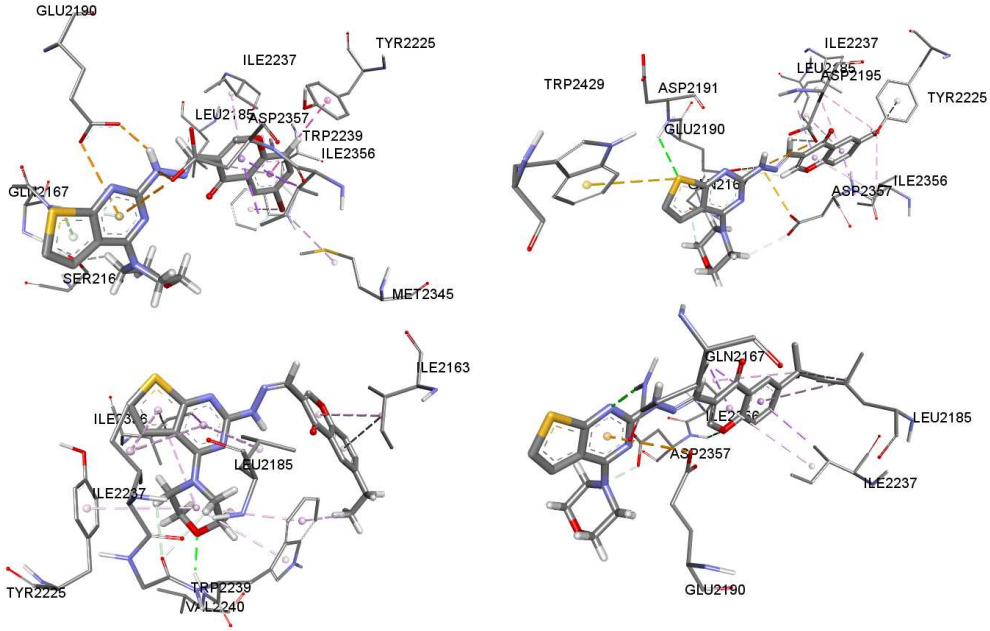

Figure 8. Docking results for molecules 13 (upper left), 14 (upper right), 15 (lower left) and 16 (lower right)

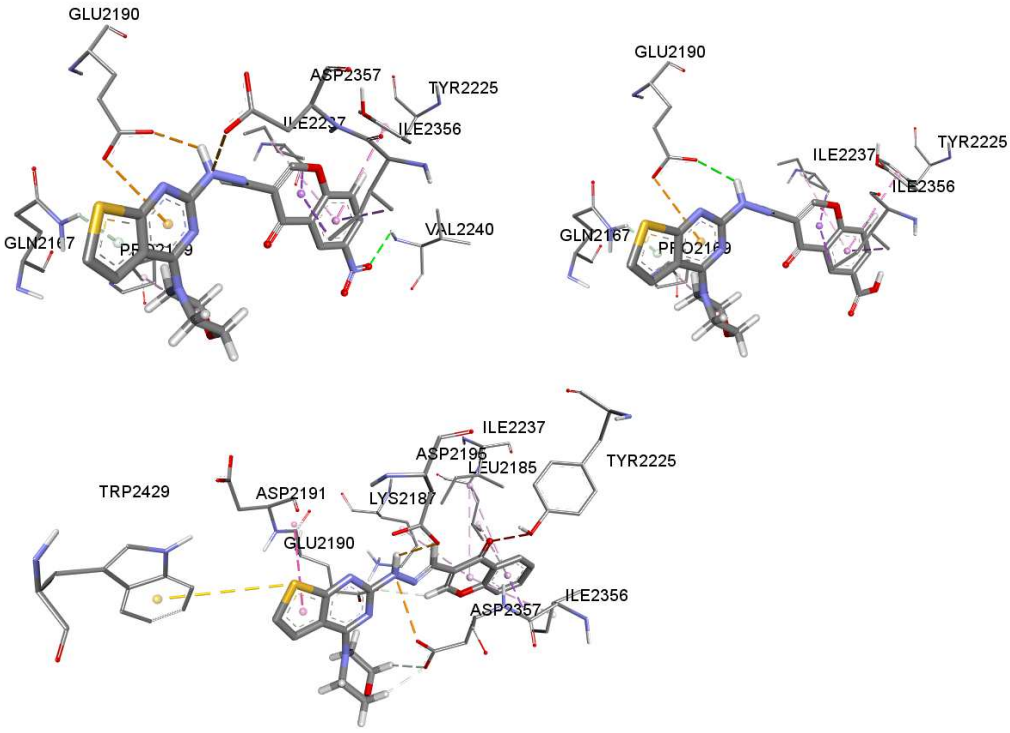

Figure 9. Docking results for molecules 17 (upper left), 18 (upper right) and 18 (lower)

Table 2. List of colors for docking figures analysis

Interaction	Color name	RGB
Pi-alkyl (hydrophobic)	Cotton candy	(255,200,255)
Alkyl (hydrophobic)	Cotton candy	(255,200,255)
Pi-sigma (hydrophobic)	Heliotrope	(200,100,255)
Carbon-hydrogen bond	Honeydew	(220,255,220)
Conventional H-bond	Lime	(0,255,0)
Salt bridge (attractive charge)	Orange peel	(255,150,0)
Pi-anion	Orange peel	(255,150,0)
Pi-Pi stacked	Neon pink	(255,100,200)
Pi-Pi T shaped	Neon pink	(255,100,200)
Halogen	Aqua	(0,255,255)
Attractive charge	Orange peel	(255,150,0)
Carbon-hydrogen bond, halogen	Honeydew	(220,255,220)
Pi-sulphur	Tangerine yellow	(255,200,0)
Unfavorable donor-donor	Red	(255,10,0)
Unfavorable positive-positive	Red	(255,10,0)
Pi-cation	Orange peel	(255,150,0)
Unfavorable acceptor-acceptor	Red	(255,10,0)

Local Molecular Orbitals

Tables 3 and 4 show the local molecular orbital structure of some atoms appearing in the QSAR result (Reading: Molecule's number (HOMO)/ (HOMO-2)*, (HOMO-1)*, (HOMO)*- (LUMO)*, (LUMO+1)*, (LUMO+2)*). Lp (lp) means lone pair.

Table 3. Local molecular orbital structure of atoms 8, 12 and 20

Mol.	Atom 8 (O)	Atom 12 (C)	Atom 20 (N)
1 (114)	109π113π114π-115π116π118π	108π109π113π-115π116π117π	112π113π114π-116π117π118π
2 (123)	120π122π123π-124π125π127π	119π120π122π-124π125π126π	121π122π123π-125π126π127π
3 (110)	107π109π110π-111π112π114π	106π107π109π-111π112π113π	108π109π110π-113π114π115π
4 (114)	111π113π114π-115π118π123π	110π111π113π-115π116π117π	112π113π114π-117π118π119π
5 (122)	119π121π122π-123π126π127π	119π121π122π-123π124π125π	120π121π122π-125π126π127π
6 (110)	108π109π110π-111π112π114π	108π109π110π-111π112π113π	107π109π110π-113π115π116π
7 (117)	112π116π117π-119π120π122π	110π111π112π-118π120π122π	115π116π117π-120π121π123π
8 (117)	112π116π117π-118π119π120π	111π112π116π-118π119π120π	115π116π117π-120π121π122π
9 (106)	101π105π106π-107π110π116π	100π101π105π-107π108π109π	104π105π106π-109π110π111π
10 (118)	115π117π118π-119π122π123π	114π115π117π-119π120π121π	116π117π118π-121π122π123π
11 (110)	107π109π110π-111π112π114π	105π107π109π-111π112π113π	108π109π110π-112π113π114π
12 (114)	111π113π114π-115π116π117π	109π111π113π-115π116π117π	112π113π114π-116π117π118π
13 (123)	120π122π123π-124π125π126π	119π120π122π-124π125π126π	121π122π123π-125π126π127π
14 (110)	107π109π110π-111π114π115π	106π107π109π-111π112π113π	108π109π110π-112π113π114π
15 (114)	112π113π114π-115π118π119π	111π112π113π-115π116π117π	111π113π114π-116π117π118π
16 (122)	119π121π122π-123π126π127π	118π119π121π-123π124π125π	120π121π122π-124π125π126π
17 (117)	115π116π117π-119π120π122π	110π111π112π-118π120π122π	115π116π117π-120π121π122π
18 (117)	114π116π117π-118π119π120π	112π114π116π-118π119π120π	115π116π117π-120π121π122π
19 (106)	103π105π106π-107π110π111π	101π103π105π-107π108π109π	104π105π106π-108π109π110π

Table 4. Local Molecular Orbital Structure of atoms 24 and 30

Mol.	Atom 24 (O)	Atom 30 (H)
1 (114)	111Ip112ip113ip-134Ip137Ip138σ	105σ110σ112σ-125σ126σ128σ
2 (123)	121Ip122Ip123Ip-140Ip143Ip146σ	111σ114σ121σ-134σ135σ137σ
3 (110)	105Ip107Ip109Ip-130Ip133σ134σ	99σ101σ108σ-121σ123σ129σ
4 (114)	109Ip111Ip113Ip-134Ip138σ140σ	103σ105σ112σ-125σ126σ127σ
5 (122)	118Ip119Ip121Ip-146Ip149Ip150σ	111σ113σ120σ-134σ135σ136σ
6 (110)	106Ip108Ip109Ip-127Ip130Ip133σ	99σ101σ107σ-121σ122σ123σ
7 (117)	115Ip116Ip117Ip-135Ip138Ip140σ	108σ113σ115σ-129σ131σ133σ
8 (117)	115Ip116Ip117Ip-138Ip141Ip143σ	106σ107σ115σ-129σ130σ131σ
9 (106)	102Ip103Ip105Ip-122Ip125Ip128σ	96σ97σ104σ-117σ118σ119σ
10 (118)	113Ip115Ip117Ip-139Ip144σ145σ	107σ109σ116σ-129σ130σ132σ
11 (110)	107Ip109Ip110Ip-129Ip134Ip135σ	99σ101σ108σ-120σ121σ122σ
12 (114)	111Ip113Ip114Ip-134Ip138Ip139σ	103σ105σ112σ-124σ125σ127σ
13 (123)	120Ip122Ip123Ip-143IP147Ip148σ	111σ114σ121σ-133σ134σ136σ
14 (110)	105Ip107Ip109Ip-130IP134Ip135σ	99σ101σ108σ-119σ120σ121σ
15 (114)	112Ip113Ip114Ip-130Ip133Ip137σ	96σ104σ105σ-123σ124σ132σ
16 (122)	119Ip121Ip122Ip-144Ip150σ151σ	111σ113σ120σ-132σ133σ134σ
17 (117)	115Ip116Ip117Ip-137Ip141Ip142σ	108σ113σ114σ-127σ128σ129σ
18 (117)	114Ip116Ip117Ip-138Ip142σ143σ	105σ107σ115σ-128σ129σ130σ
19 (106)	103Ip105Ip106Ip-125Ip129Ip130σ	95σ97σ104σ-115σ116σ117σ

LMRA results

The best equation obtained was:

$$\log(\text{inhibitory \% at } 10\mu\text{M}) = 1.23 + 3.53F_{12}(\text{LUMO})^* + 0.13F_{30}(\text{LUMO+1})^* \\ -0.00007S_8^N(\text{LUMO+2})^* + 1.32S_{24}^N(\text{LUMO+2})^* - 0.003S_{20}^N(\text{LUMO+2})^* \quad (2)$$

with R= 0.99, R^2= 0.97, adj-R^2= 0.97, F(5,12)=84.345 ($p<0.000001$) and a standard error of estimate of 0.03. No outliers were detected and no residuals fall outside the ±2σ limits. Here, $F_{12}(\text{LUMO})^*$ is the Fukui index (i.e., the electron population) of the lowest empty MO localized on atom 12, $F_{30}(\text{LUMO+1})^*$ is the Fukui index of the second lowest empty MO localized on atom 30, $S_8^N(\text{LUMO+2})^*$ is the nucleophilic superdelocalizability of the third lowest MO localized on atom 8, $S_{24}^N(\text{LUMO+2})^*$ is the nucleophilic superdelocalizability of the third lowest MO localized on atom 24 and $S_{20}^N(\text{LUMO+2})^*$ is the nucleophilic superdelocalizability of the third lowest MO localized on atom 20. Table 5 shows the beta coefficients and the results of the t-test for significance of

coefficients of Eq. 2. Table 6 displays the squared correlation coefficients for the variables appearing in Eq. 2, showing that there are no significant internal correlations. Fig. 10 displays the plot of observed *vs.* calculated $\log(\text{inhibitory \% at } 10\mu\text{M})$ values. The associated statistical parameters of Eq. 2 indicate that this equation is statistically significant and that the variation of the numerical value of a group of five local atomic reactivity indices of atoms of the common skeleton explains about 97% of the variation of the inhibitory percentage.

Table 5. Beta coefficients and t-test for significance of coefficients in Eq. 2

Variable	Beta	t(12)	p-level
$F_{12}(\text{LUMO})^*$	0.94	18.28	<0.0000001
$F_{30}(\text{LUMO+1})^*$	0.21	3.82	<0.002
$S_8^N(\text{LUMO+2})^*$	-0.42	-8.01	<0.000004
$S_{24}^N(\text{LUMO+2})^*$	0.38	7.07	<0.00001
$S_{20}^N(\text{LUMO+2})^*$	-0.28	-4.66	<0.0006

Table 6. Matrix of squared correlation coefficients for the variables in Eq. 2

	$F_{12}(\text{LUMO})^*$	$F_{30}(\text{LUMO+1})^*$	$S_8^N(\text{LUMO+2})^*$	$S_{24}^N(\text{LUMO+2})^*$
$F_{30}(\text{LUMO+1})^*$	0.0	1.00		
$S_8^N(\text{LUMO+2})^*$	0.02	0.01	1.00	
$S_{24}^N(\text{LUMO+2})^*$	0.002	0.04	0.002	1.00
$S_{20}^N(\text{LUMO+2})^*$	0.06	0.14	0.04	0.02

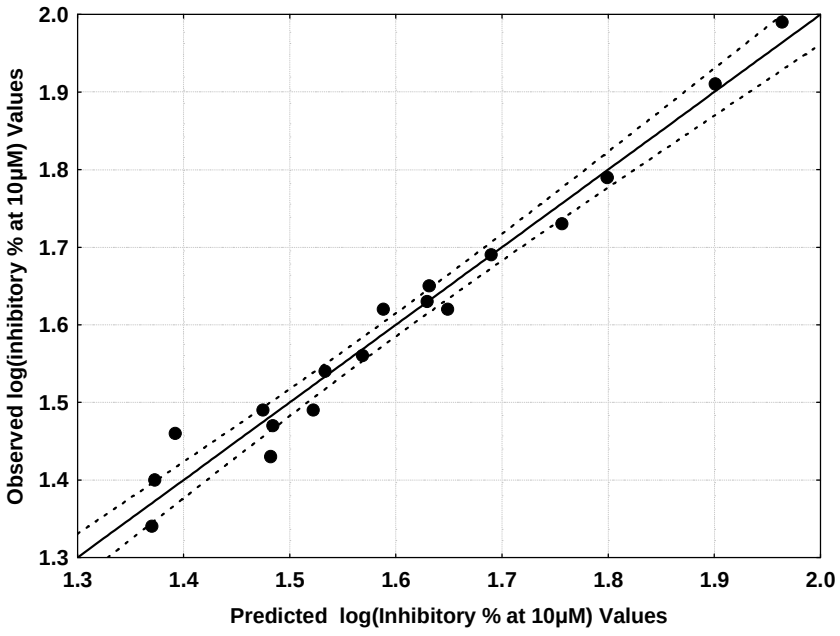

Figure 10. Observed *vs.* calculated $\log(10\ \mu\text{M inhibitory \%})$ values. Dashed lines denote the 95% confidence interval

DISCUSSION

Docking results

Table 7 shows the kinds, partners and distances of the interactions (see also Fig. 3).

Table 7. Summary of intramolecular interactions of thienopyrimidine derivatives with the mTOR binding site from Figs. 5-9

Mol.	Interactions
1	Alkyl interaction between Cl with Ile-2356 (4.36 Å) and Ile-2237 (5.23 Å), π-alkyl interaction of Cl and Tyr-2225 (4.43 Å), π-alkyl interaction between ring A with Leu-2185 (5.42 Å) and Ile-2237 (4.55 Å), π-σ interaction of ring A with Ile-2356 (3.74 Å), π-alkyl interaction between ring B with Ile-2356 (4.97 Å), π-σ interaction of ring B with Ile-2237 (3.95 Å), carbon H-bond interaction of C9-H with Glu-2190 (2.51 Å), carbon H-bond interaction of C3-H with Asp-2195 (2.39 Å), attractive charge interaction of N2 with Asp-2357 (3.57Å) and Glu-2190 (3.83Å), salt bridge, attractive charge interaction of H31 and Asp-2195 (2.99Å and 2.97Å), π-anion interaction of ring C and Asp-2357 (3.97 Å), carbon H-bond interaction between C25-H with Gln-2167 (2.54Å) and carbon H-bond interaction of C23-H and Asp-2357 (2.37 Å).
2	Alkyl interaction between Br and Ile-2356 (4.62 Å), π-alkyl interaction of Br and Tyr-2225 (4.31 Å), π-alkyl interaction between ring A with Leu-2185 (5.33 Å) and Ile-2237 (4.57 Å), π-σ interaction of ring A with Ile-2356 (3.77 Å), π-alkyl interaction of ring B with Lys-2187 (5.48 Å) and Ile-2356 (4.79 Å), π-σ interaction of ring B with Ile-2237 (3.85 Å), carbon H-bond interaction of C9-H and Glu-2190 (2.71 Å), attractive charge interaction between N2 with Asp-2357 (3.41 Å), Glu-2190 (3.63 Å) and Asp-2195 (3.82 Å), carbon H-bond of C3-H and Asp-2195 (2.43 Å), π-anion interaction of ring C and Glu-2190 (4.04 Å) and carbon H-bond interaction between C25-H and Lys-2187 (3.04 Å and 3.05 Å).
3	Alkyl interaction between methyl substituent of ring A with Ile-2356 (4.51 Å) and Ile-2237 (5.29 Å), π-alkyl interaction between methyl substituent of ring A and Tyr-2225 (4.35 Å), π-alkyl interaction of ring A with Leu-2185 (5.36 Å) and Ile-2237 (4.58 Å), π-σ interaction of ring A and Ile-2356 (3.75 Å), π-σ interaction between ring B and Ile-2237 (3.96 Å), π-alkyl interaction of ring B and Ile-2356 (4.71 Å), carbon H-bond interaction of C9-H and Glu-2190 (2.84 Å), carbon H-bond interaction of C3-H and Asp-2195 (2.42 Å), attractive charge interaction between N2 with Glu-2190 (3.64 Å) and Asp-2357 (3.31 Å), salt bridge; attractive charge interaction of H31 and Asp-2195 (3.15 Å), carbon H-bond interaction of C23-H and Asp-2357 (2.43 Å), carbon H-bond interaction between C26-H and Gln-2167 (2.99 Å) and π-anion interaction of ring C and Glu-2190 (4.01 Å)
4	π-alkyl interaction between ethyl substituent of ring A and Trp-2239 (4.30 Å and 4.31 Å), alkyl interaction between ethyl substituent of ring A with Leu-2185 (5.08 Å), π-alkyl interaction of ring A with Leu-2185 (5.00 Å) and Ile-2237 (5.22 Å), π-σ interaction of ring A and Ile-2356 (3.50 Å), π-alkyl interaction of ring B with Ile-2356 (4.68 Å), Lys-2187 (5.41 Å) and Ile-2237 (4.79 Å), unfavorable acceptor-acceptor interaction of O10 and Tyr-2225 (2.87 Å), carbon H-bond interaction of C9-H and Glu-2190 (2.74 Å), attractive charge interaction between N2 with Glu-2190 (3.61 Å) and Asp-2357 (3.38 Å), salt bridge; attractive charge interaction of H31 and Asp-2195 (2.81 Å), carbon H-bond interaction of C23-H and Gln-2167 (2.82 Å), π-sulfur interaction of S27 with Trp-2429 (5.93 Å), π-anion interaction between ring C with Glu-2190 (3.93Å) and carbon H-bond interaction of C22-H with Asp-2357 (2.93Å).
5	Alkyl interaction between the *t*-butyl substituent of ring A with Ile-2356 (4.72Å), Met-2345 (5.47Å) and Leu-2185 (5.38Å), π-σ interaction between the *t*-butyl substituent of ring A with Trp-2239 (3.61Å), π-alkyl interaction of ring A with Leu-2185 (5.49Å) and Ile2237 (4.64Å), π-σ interaction between ring A and Ile-2356 (3.69Å), π-alkyl interaction of ring B with Ile-2237 (5.41Å), π-σ interaction between ring B and Ile-2356 (3.79Å), conventional H-bond interaction between O8 with HN of Asp-2357 (2.61Å), carbon H-bond interaction between N1 with HE1 and HE2 of Lys-2187 (2.76Å and 2.87Å), salt bridge; attractive charge interaction of H31 with OE2 of Glu-2190 (2.85Å), conventional H-bond interaction between N20 with HE21 of Gln-2167 (2.77Å), carbon H-bond interaction of C22-H with O10 (2.79Å), carbon H-bond interaction of C25-H with O10 (3.03Å) and carbon H-bond interaction of C26-H with O10 (2.67Å).
6	π-alkyl interaction of ring A with Leu-2185 (5.31 Å) and Ile-2237 (4.70 Å), π-σ interaction of ring A and Ile-2356 (3.64 Å), π-alkyl interaction of ring B with Ile-2356 (4.83 Å) and Lys-2187 (5.48 Å), π-σ interaction between ring B and Ile-2237 (3.96 Å), carbon H-bond interaction of C9-H and Glu-2190 (2.60 Å), carbon H-bond of C3-H and Asp-2195 (2.50 Å), attractive charge interaction of N2 with Asp-2195 (3.80 Å), Glu-2190 (3.71 Å) and Asp-2357 (3.58 Å), π-anion interaction of ring C and Asp-2357 (3.83 Å), carbon H-bond interaction of C23-H with Asp-2357 (2.40 Å) and carbon H-bond interaction of C25-H and Gln-2167 (2.57Å).
7	Conventional H-bond between the nitro substituent of ring A and Val-2240 (2.66 Å), π-π T-shaped interaction of ring A with Tyr-2225 (5.04 Å), π-σ interaction of ring A and Ile-2356 (3.66 Å), π-alkyl interaction of ring A with Ile-2237 (5.28 Å), π-σ interaction between ring B with Ile-2237 (3.95 Å) and Ile-2356 (3.81 Å), π-alkyl interaction of ring B and Leu-2185 (5.49 Å), salt bridge; attractive charge interaction of H31 and Glu-2190 (2.62 Å), attractive charge interaction between N2 and Asp-2357 (3.36 Å), π-anion interaction of ring C and Glu-2190 (4.69 Å) and alkyl interaction of ring D with Pro-2169 (5.37 Å).
8	π-alkyl interaction of ring A with Leu-2185 (5.22 Å) and Ile-2237 (4.72 Å), π-σ interaction of ring A with Ile-2356 (3.69 Å), π-alkyl interaction of ring B with Ile-2356 (4.81 Å) and Lys-2187 (5.38 Å), π-σ interaction between ring B with Ile-2237 (3.82 Å), carbon H-bond interaction of C9-H and Glu-2190 (2.66 Å), π-anion interaction between ring C and Glu-2190 (3.98 Å), carbon H-bond interaction of C25-H with Gln-2167 (2.84 Å) and carbon H-bond interaction of C26-H with Asp-2357 (2.72Å).
9	π-alkyl interaction of ring A with Leu-2185 (5.04 Å) and Ile-2237 (5.20 Å), π-σ interaction of ring A with Ile-2356 (3.48 Å), π-alkyl interaction of ring B with Ile-2356 (4.78 Å), Lys-2187 (5.35 Å) and Ile-2237 (4.74 Å), carbon H-bond between C9-H and Glu-2190 (2.57 Å), salt bridge; attractive charge interaction of H31 and Asp-2195 (2.61 Å), attractive charge interaction between N2 with Asp-2357 (3.48 Å) and Glu-2190 (3.96 Å) and π-anion interaction between ring C with Asp-2357 (3.68 Å), and carbon H-bond interaction between C26-H and Asp-2357 (2.42Å).
10	Alkyl interaction between the isopropyl substituent of ring A with Leu-2185 (4.46 Å), Ile-2356 (4.65 Å) and Ile-2237 (5.39 Å and 5.23 Å), π-alkyl interaction between the isopropyl substituent of ring A with Tyr-2225 (3.78 Å) and Trp-2239 (4.55 Å and 4.26 Å), π-alkyl interaction of ring A with Leu-2185 (5.20 Å) and Ile-2237 (4.85 Å), π-σ interaction of ring A with Ile-2356 (3.60 Å), π-alkyl interaction of ring B with Ile-2356 (4.82 Å) and Ile-2237 (4.85 Å), carbon H-bond interaction of C9-H and Glu-2190 (2.67 Å), attractive charge

	interaction between N2 with Asp-2357 (3.85 Å), Asp-2195 (3.65 Å) and Glu-2190 (3.82 Å), π-anion interaction of ring C with Asp-2357 (3.76 Å), carbon H-bond of C3-H with Asp-2195 (2.90 Å and 2.21 Å) and carbon H-bond interaction between C22-H and Asp-2357 (2.65Å).
11	π-π T-shaped interaction of ring A with Tyr-2225 (5.21 Å), π-σ interaction of ring A with Ile-2356 (3.93 Å), π-σ interaction of ring B with Ile-2356 (3.75 Å and 3.80 Å) and Ile-2237 (3.88 Å), carbon H-bond interaction between O10 and C25-H (2.74 Å), salt bridge; attractive charge interaction of H31 and Glu-2190 (2.14 Å), attractive charge interaction between N2 with Asp-2357 (4.67 Å), carbon H-bond between C22-H with Ser-2165 (2.65 Å) and π-donor H-bond interaction of ring E and Gln-2167 (3.04 Å).
12	π-anion interaction of ring B with Glu-2190 (4.51 Å), attractive charge interaction between N2 with Asp-2357 (3.78 Å) and Glu-2190 (4.15 Å), salt bridge; attractive charge interaction of H31 and Asp-2195 (2.12 Å), π-alkyl interaction of ring C with Ile-2356 (4.84 Å) and Ile-2237 (5.07 Å), carbon H-bond interaction between C25-H with Glu-2190 (3.02 Å and 2.92 Å), π-alkyl interaction of ring E with Ile-2237 (4.63 Å), π-σ interaction of ring E with Ile-2356 (3.69 Å), carbon H-bond interaction of C3-H with Asp-2357 (2.61Å) and Asp-2195 (2.93Å), carbon H-bond interaction of C23-H with Asp-2357 (2.34Å) and carbon H-bond interaction of C22-H with Asn-2343 (2.97Å).
13	π-alkyl interaction of Br and Trp-2239 (3.77 Å and 3.90 Å), alkyl interaction of Br and Met-2345 (4.99 Å), π-π T-shaped interaction of ring A with Tyr-2225 (5.14 Å), π-σ interaction of ring A with Ile-2237 (3.98 Å) and Ile-2356 (3.65 Å), π-alkyl interaction of ring A with Leu-2185 (5.43 Å), π-σ interaction of ring B with Ile-2356 (3.87 Å and 3.79 Å), π-alkyl interaction of ring B and Ile-2237 (4.40 Å), salt bridge; attractive charge interaction of H31 and Glu-2190 (2.30 Å), attractive charge interaction between N2 with Asp-2357 (3.26 Å), π-anion interaction of ring C with Asp-2357 (3.97 Å) and Glu-2190 (4.55 Å), π-donor H-bond interaction of ring C and Gln-2167 (2.90 Å), π-donor H-bond interaction of ring E and Gln-2167 (2.54 Å) and carbon H-bond interaction between C3-H and Ser-2165 (2.76 Å).
14	π-alkyl interaction between the methyl substituent of ring A with Tyr-2225 (4.34 Å), alkyl interaction between the methyl substituent of ring A with Ile-2356 (4.49 Å) and Ile-2237 (5.34 Å), π-σ interaction of ring A with Ile-2356 (3.76 Å), π-alkyl interaction of ring A with Ile-2237 (4.58 Å) and Leu-2185 (5.35 Å), π-σ interaction of ring B and Ile-2237 (3.91 Å), π-alkyl interaction between ring B and Ile-2356 (4.73 Å), carbon H-bond interaction between C9-H and Glu-2190 (2.80 Å), carbon H-bond interaction between C3-H and Asp-2195 (2.78 Å), attractive charge interaction between N2 with Asp-2357 (3.33 Å), Asp-2195 (3.81 Å) and Glu-2190 (3.66 Å), carbon H-bond interaction between C26-H and Gln-2167 (3.02 Å), carbon H-bond interaction between C22-H with Asp-2357 (2.83Å), carbon H-bond interaction of C25-H with Gln-2167 (2.80Å), conventional H-bond interaction between S and Asp-2191 (2.95 Å) and π-Sulfur interaction of S and Trp-2429 (5.08 Å).
15	Π-alkyl interaction between the ethyl substituent of ring A and Trp-2239 (5.19Å), π-alkyl interaction between ring A and Ile-2163 (4.99 Å), π-alkyl interaction between ring B with Ile-2163 (4.83Å), π-σ interaction of ring C with Ile-2356 (4.16 Å) and Ile-2237(4.30Å), π-alkyl interaction between Tyr-2225 (5.06Å) and Trp-2239 (5.38Å and 5.17Å), alkyl interaction of ring D with Ile-2356 (5.22Å), conventional H-bond interaction of O24 and Val-2240 (2.08Å), carbon H-bond interaction between C22-H with Gly-2238 (2.95Å) and carbon H-bond interaction between C26-H and Gly-2238 (2.88Å).
16	Alkyl interaction between t-butyl substituent of ring A with Ile-2356 (4.96 Å) and Leu-2185 (5.15 Å), π-σ interaction of ring A with Ile-2237 (3.91 Å) and Ile-2356 (3.80 Å), π-alkyl interaction of ring A with Leu-2185 (5.45 Å), π-alkyl interaction of ring B with Ile-2237 (5.33 Å), π-σ interaction of ring B with Ile-2356 (3.84 Å), conventional H-bond interaction of O8 with Asp-2357 (2.71 Å), conventional H-bond interaction of N20 and Gln-2167 (2.05 Å), π-anion interaction of ring C with Glu-2190 (4.21 Å) and carbon H-bond interaction between C23-H and Asp-2357 (2.52 Å).
17	Conventional H-bond between the nitro substituent of ring A with Val-2240 (2.70 Å), π-π T-shaped interaction of ring A with Tyr-2225 (5.03 Å), π-alkyl interaction of ring A with Ile-2237 (5.28 Å), π-σ interaction of ring A with Ile-2356 (3.65 Å), π-σ interaction of ring B with Ile-2356 (3.83 Å) and Ile-2237 (3.93 Å), salt bridge; attractive charge interaction of H31 and Glu-2190 (2.70 Å), attractive charge interaction between N2 with Asp-2357 (3.32 Å), π-anion interaction of ring C and Glu-2190 (4.64 Å), π-donor H-bond interaction between ring D with Gln-2167 (2.56 Å) and alkyl interaction between ring E and Pro-2169 (5.35 Å).
18	π-π T-shaped interaction of ring A with Tyr-2225 (5.08 Å), π-alkyl interaction of ring A with Ile-2237 (5.40 Å), π-σ interaction of ring A with Ile-2356 (3.65 Å), π-σ interaction of ring B with Ile-2356 (3.82 Å) and Ile-2237 (3.91 Å), conventional H-bond interaction between H31 and Glu-2190 (2.73 Å), alkyl interaction between ring D and Pro-2169 (5.38 Å), π-donor H-bond interaction between ring E with Gln-2167 (2.54 Å) and π-anion interaction of ring C and Glu-2190 (4.64 Å).
19	π-alkyl interaction of ring A with Leu-2185 (5.02 Å) and Ile-2237 (5.29 Å), π-σ interaction of ring A with Ile-2356 (3.45 Å), π-alkyl interaction of ring B with Ile-2356 (4.67 Å), Ile-2237 (4.83 Å) and Lys-2187 (5.44 Å), unfavorable acceptor-acceptor interaction of O10 and Tyr-2225 (2.84 Å), carbon H-bond interaction between C9-H and Glu-2190 (2,71 Å), carbon H-bond interaction of C3-H with Asp-2195 (3.06Å), salt bridge; attractive charge interaction of H31 and Asp-2195 (2.66 Å), attractive charge interaction between N2 with Asp-2357 (3.43 Å) and Glu-2190 (3.80 Å), carbon H-bond interaction between C23-H with Asp-2357 (2.29 Å), carbon H-bond interaction of C26-H with Asp-2357 (2.55Å), amide-π stacked interaction of ring E with Glu-2190 (5.39 Å) and π-sulfur interaction of S and Trp-2429 (5.54 Å).

The amino acids participating in the ligand-site interaction are shown in Table 8.

Table 8. Summary of the amino acids participating in the ligand-site interaction

Mol.	Amino acids.
1	Asp-2195, Asp-2357, Gln-2167, Glu-2190, Ile-2237, Ile-2356, Leu-2185, Tyr-2225.
2	Asp-2195, Asp-2357, Gln-2167, Glu-2190, Ile-2237, Ile-2356, Leu-2185, Lys-2187, Tyr-2225.
3	Asp-2195, Asp-2357, Gln-2167, Glu-2190, Ile-2237, Ile-2356, Leu-2185, Tyr-2225.
4	Asp-2195, Asp-2357, Gln-2167, Glu-2190, Ile-2237, Ile-2356, Leu-2185, Lys-2187, Trp-2239, Trp-2429, Tyr-2225.
5	Asp-2357, Gln-2167, Glu-2190, Ile2237, Ile-2356, Leu-2185, Lys-2187, Met-2345, Trp-2239.
6	Asp-2195, Asp-2357, Gln-2167, Glu-2190, Ile-2237, Ile-2356, Leu-2185, Lys-2187.
7	Asp-2357, Glu-2190, Ile-2237, Ile-2356, Leu-2185, Pro-2169, Tyr-2225, Val-2240.
8	Asp-2357, Gln-2167, Glu-2190, Ile-2237, Ile-2356, Leu-2185, Lys-2187.
9	Asp-2195, Asp-2357, Glu-2190, Ile-2237, Ile-2356, Leu-2185, Lys-2187.
10	Asp-2195, Asp-2357, Glu-2190, Ile-2237, Ile-2356, Leu-2185, Trp-2239, Tyr-2225.
11	Asp-2357, Gln-2167, Glu-2190, Ile-2237, Ile-2356, Ser-2165, Tyr-2225.
12	Asn-2343, Asp-2195, Asp-2357, Glu-2190, Ile-2237, Ile-2356.
13	Asp-2357, Gln-2167, Glu-2190, Ile-2237, Ile-2356, Leu-2185, Met-2345, Ser-2165, Trp-2239, Tyr-2225.
14	Asp-2191, Asp-2195, Asp-2357, Gln-2167, Glu-2190, Ile-2237, Ile-2356, Leu-2185, Trp-2429, Tyr-2225.
15	Ile-2163, Ile-2237, Ile-2356, Leu-2185, Trp-2239, Tyr-2225, Val-2240.
16	Asp-2357, Ile-2237, Ile-2356, Gln-2167, Glu-2190, Leu-2185.
17	Asp-2357, Gln-2167, Glu-2190, Ile-2237, Ile-2356, Pro-2169, Tyr-2225, Val-2240.
18	Ile-2237, Ile-2356, Gln-2167, Glu-2190, Pro-2169, Tyr-2225.
19	Asp-2195, Asp-2357, Glu-2190, Ile-2237, Ile-2356, Leu-2185, Lys-2187, Trp-2429, Tyr-2225.

From Table 8 we can see that the amino acid percentage appearing as interaction partners is: Ile-2237 and Ile-2356 in 100% of cases, Glu-2190 in 94.74%, Asp-3257 in 84.21%, Leu-2185 in 78.95%, Tyr-2225 and Gln-2167 in 68.42 %, Asp-2195 in 47.37%, Lys-2187 and Trp-2239 in 36.84% of cases. Other amino acids appear in smaller percentages (Pro-2169 and Val-2240 in 15.79% of cases, Met-2345, Trp-2429 and Ser-2165 in 10.53%, Ala-2248 and Asp-2191 in 5.26% of cases). An acceptable conclusion is that the molecules analyzed here share the same binding site. For a better analysis, and like in previous works, we used Table 7 to classify the ligand-site interactions in short- (d≤3Å), medium- and long-range (d>5Å) ones. Table 9 shows the short-range interactions.

Table 9. Short-range ligand-site interactions (d≤3Å)

Mol.	Interactions
1	Carbon H-bond interaction of C9-H with Glu-2190 (2.51 Å), carbon H-bond interaction of C3-H with Asp-2195 (2.39 Å), salt bridge, attractive charge interaction of H31 and Asp-2195 (2.99Å and 2.97Å), carbon H-bond interaction between C25-H with Gln-2167 (2.54Å) and carbon H-bond interaction of C23-H and Asp-2357 (2.37 Å).
2	Carbon H-bond interaction of C9-H and Glu-2190 (2.71 Å), carbon H-bond of C3-H and Asp-2195 (2.43 Å), carbon H-bond interaction between C25-H and Gln-2167 (3.04 Å and 3.05 Å).
3	Carbon H-bond interaction of C9-H and Glu-2190 (2.84 Å), carbon H-bond interaction of C3-H and Asp-2195 (2.42 Å), carbon H-bond interaction of C23-H and Asp-2357 (2.43 Å), carbon H-bond interaction between C26-H and Gln-2167 (2.99 Å).
4	Unfavorable acceptor-acceptor interaction of O10 and Tyr-2225 (2.87 Å), carbon H-bond interaction of C9-H and Glu-2190 (2.74 Å), salt bridge; attractive charge interaction of H31 and Asp-2195 (2.81 Å), carbon H-bond interaction of C23-H and Gln-2167 (2.82 Å) and carbon H-bond interaction of C22-H with Asp-2357 (2.93Å).
5	Conventional H-bond interaction between O8 with HN of Asp-2357 (2.61Å), carbon H-bond interaction between N1 with HE1 and HE2 of Lys-2187 (2.76Å and 2.87Å), salt bridge; attractive charge interaction of H31 with OE2 of Glu-2190 (2.85Å), conventional H-bond interaction between N20 with HE21 of Gln-2167 (2.77Å), carbon H-bond interaction of C22-H with O10 (2.79Å), carbon H-bond interaction of C25-H with O10 (3.03Å) and carbon H-bond interaction of C26-H with O10 (2.67Å).
6	Carbon H-bond interaction of C9-H and Glu-2190 (2.60 Å), carbon H-bond of C3-H and Asp-2195 (2.50 Å), carbon H-bond interaction of C23-H with Asp-2357 (2.40 Å) and carbon H-bond interaction of C25-H and Gln-2167 (2.57Å).
7	Conventional H-bond between the nitro substituent of ring A and Val-2240 (2.66 Å), salt bridge; attractive charge interaction of H31 and Glu-2190 (2.62 Å).
8	Carbon H-bond interaction of C9-H and Glu-2190 (2.66 Å), carbon H-bond interaction of C25-H with Gln-2167 (2.84 Å) and carbon H-bond interaction of C26-H with Asp-2357 (2.72Å).
9	Carbon H-bond between C9-H and Glu-2190 (2.57 Å), salt bridge; attractive charge interaction of H31 and Asp-2195 (2.61 Å), and carbon H-bond interaction between C26-H and Asp-2357 (2.42Å).
10	Carbon H-bond interaction of C9-H and Glu-2190 (2.67 Å), carbon H-bond of C3-H with Asp-2195 (2.90 Å and 2.72 Å) and carbon H-bond interaction between C22-H and Asp-2357 (2.65Å).
11	Carbon H-bond interaction between O10 and C25-H (2.74 Å), salt bridge; attractive charge interaction of H31 and Glu-2190 (2.14 Å), carbon H-bond between C22-H and Ser-2165 (2.65 Å) and π-donor H-bond interaction of ring E and Gln-2167 (3.04 Å)..
12	Salt bridge; attractive charge interaction of H31 and Asp-2195 (2.12 Å), carbon H-bond interaction between C25-H with Glu-2190 (3.02 Å and 2.92 Å), carbon H-bond interaction of C3-H with Asp-2357 (2.61Å) and Asp-2195 (2.93Å), carbon H-bond interaction of C23-H with Asp-2357 (2.34Å) and carbon H-bond interaction of C22-H with Asn-2343 (2.97Å).
13	Salt bridge; attractive charge interaction of H31 and Glu-2190 (2.30 Å), π-donor H-bond interaction of ring C and Gln-2167 (2.90 Å), π-donor H-bond interaction of ring E and Gln-2167 (2.54 Å) and carbon H-bond interaction between C3-H and Ser-2165 (2.76 Å).
14	Carbon H-bond interaction between C9-H and Glu-2190 (2.80 Å), carbon H-bond interaction between C3-H and Asp-2195 (2.78 Å),

	carbon H-bond interaction between C26-H and Gln-2167 (3.02 Å), carbon H-bond interaction between C22-H with Asp-2357 (2.83Å), carbon H-bond interaction of C25-H with Gln-2167 (2.80Å), conventional H-bond interaction between S and Asp-2191 (2.95 Å)
15	H-bond interaction of O24 and Val-2240 (2.08Å), carbon H-bond interaction between C22-H with Gly-2238 (2.95Å) and carbon H-bond interaction between C26-H and Gly-2238 (2.88Å).
16	Conventional H-bond interaction of O8 with Asp-2357 (2.71 Å), conventional H-bond interaction of N20 and Gln-2167 (2.05 Å) and carbon H-bond interaction between C23-H and Asp-2357 (2.52 Å).
17	Conventional H-bond between the nitro substituent of ring A with Val-2240 (2.70 Å), salt bridge; attractive charge interaction of H31 and Glu-2190 (2.70 Å), π-donor H-bond interaction between ring D with Gln-2167 (2.56 Å)
18	Conventional H-bond interaction between H31 and Glu-2190 (2.73 Å), π-donor H-bond interaction between ring E with Gln-2167 (2.54 Å)
19	Unfavorable acceptor-acceptor interaction of O10 and Tyr-2225 (2.84 Å), carbon H-bond interaction between C9-H and Glu-2190 (2,71 Å), carbon H-bond interaction of C3-H with Asp-2195 (3.06Å), salt bridge; attractive charge interaction of H31 and Asp-2195 (2.66 Å), carbon H-bond interaction between C23-H with Asp-2357 (2.29 Å), carbon H-bond interaction of C26-H with Asp-2357 (2.55Å).

We can see that the predominating interaction in almost all molecules is the carbon H-bond interaction of the form C-H….O. This bond is rather weak [156, 157]. The number of these contacts indicates that they play a role in stabilizing the ligand-site complex. In some molecules this kind of interaction seems to be the only one present at distances d≤3Å. Note that in other cases this kind of carbon H-bond is not present or is not the main short-range interaction [121, 122, 158, 159]. Table 10 shows the long-range interactions.

Table 10. Long-range ligand-site interactions (d>5Å)

Mol.	Interactions
1	Alkyl interaction between Cl with Ile-2237 (5.23 Å), π-alkyl interaction between ring A with Leu-2185 (5.42 Å), π-alkyl interaction between ring B and Ile-2356 (4.97 Å).
2	π-alkyl interaction between ring A with Leu-2185 (5.33 Å), π-alkyl interaction of ring B with Lys-2187 (5.48 Å).
3	Alkyl interaction between the methyl substituent of ring A with Ile-2237 (5.29 Å), π-alkyl interaction of ring A with Leu-2185 (5.36 Å).
4	Alkyl interaction between the ethyl substituent of ring A with Leu-2185 (5.08 Å), π-alkyl interaction of ring A with Leu-2185 (5.00 Å) and Ile-2237 (5.22 Å), π-alkyl interaction of ring B with Lys-2187 (5.41 Å) and π-sulfur interaction of S27 with Trp-2429 (5.93 Å).
5	Alkyl interaction between *t*-butyl substituent of ring A with Met-2345 (5.47Å) and Leu-2185 (5.38Å), π-alkyl interaction of ring A with Leu-2185 (5.49Å), π-alkyl interaction of ring B with Ile-2237 (5.41Å).
6	π-alkyl interaction of ring A with Leu-2185 (5.31 Å), π-alkyl interaction of ring B with Lys-2187 (5.48 Å).
7	π-π T-shaped interaction of ring A with Tyr-2225 (5.04 Å), π-alkyl interaction of ring A with Ile-2237 (5.28 Å), π-alkyl interaction of ring B and Leu-2185 (5.49 Å), alkyl interaction of ring D with Pro-2169 (5.37 Å).
8	π-alkyl interaction of ring A with Leu-2185 (5.22 Å), π-alkyl interaction of ring B with Lys-2187 (5.38 Å).
9	π-alkyl interaction of ring A with Leu-2185 (5.04 Å) and Ile-2237 (5.20 Å), π-alkyl interaction of ring B with Lys-2187 (5.35 Å).
10	Alkyl interaction between the isopropyl substituent of ring A with Ile-2237 (5.39 Å and 5.23 Å), π-alkyl interaction of ring A with Leu-2185 (5.20 Å).
11	π-π T-shaped interaction of ring A with Tyr-2225 (5.21 Å).
12	π-alkyl interaction of ring C with Ile-2237 (5.07 Å).
13	Alkyl interaction of Br and Met-2345 (4.99 Å), π-π T-shaped interaction of ring A with Tyr-2225 (5.14 Å), π-alkyl interaction of ring A with Leu-2185 (5.43 Å).
14	Alkyl interaction between the methyl substituent of ring A with Ile-2237 (5.34 Å), π-alkyl interaction of ring A with Leu-2185 (5.35 Å), π-sulfur interaction of S and Trp-2429 (5.08 Å).
15	π-alkyl interaction between the ethyl substituent of ring A and Trp-2239 (5.19Å), π-alkyl interaction between ring A and Ile-2163 (4.99 Å), π-alkyl interaction between Tyr-2225 (5.06Å) and Trp-2239 (5.38Å and 5.17Å), alkyl interaction of ring D with Ile-2356 (5.22Å).
16	Alkyl interaction between the isopropyl substituent of ring A with Ile-2356 (4.96 Å) and Leu-2185 (5.15 Å), π-alkyl interaction of ring A with Leu-2185 (5.45 Å), π-alkyl interaction of ring B with Ile-2237 (5.33 Å).
17	π-π T-shaped interaction of ring A with Tyr-2225 (5.03 Å), π-alkyl interaction of ring A with Ile-2237 (5.28 Å), alkyl interaction between ring E and Pro-2169 (5.35 Å).
18	π-π T-shaped interaction of ring A with Tyr-2225 (5.08 Å), π-alkyl interaction of ring A with Ile-2237 (5.40 Å), alkyl interaction between ring D and Pro-2169 (5.38 Å).
19	π-alkyl interaction of ring A with Leu-2185 (5.02 Å) and Ile-2237 (5.29 Å), π-alkyl interaction of ring B with Lys-2187 (5.44 Å), amide-π stacked interaction of ring E with Glu-2190 (5.39 Å) and π-sulfur interaction of S and Trp-2429 (5.54 Å).

We can see in Table 10 that long-range interactions are of π-π, π-σ and σ-σ that do not involve charge transfer. Within a static approach in which only the influence of the closer amino acids participating in the ligand-site interaction is considered, these interactions can be viewed as the ones involved in the long-range orientation and guiding of the ligand. Table 11 shows the interactions of the substituents that do not belong to the common skeleton with the site.

Table 11. Substituent-site interactions

Mol.	Interactions.
1	Alkyl interaction between Cl with Ile-2356 (4.36 Å) and Ile-2237 (5.23 Å), π-alkyl interaction of Cl and Tyr-2225 (4.43 Å).
2	Alkyl interaction between Br and Ile-2356 (4.62 Å), π-alkyl interaction of Br and Tyr-2225 (4.31 Å).
3	Alkyl interaction between the methyl substituent of ring A with Ile-2356 (4.51 Å) and Ile-2237 (5.29 Å), π-alkyl interaction between the methyl substituent of ring A and Tyr-2225 (4.35 Å).
4	π-alkyl interaction between the ethyl substituent of ring A and Trp-2239 (4.30 Å and 4.31 Å), alkyl interaction between the ethyl substituent of ring A with Leu-2185 (5.08 Å).
5	Alkyl interaction between the *t*-butyl substituent of ring A with Ile-2356 (4.72Å), Met-2345 (5.47Å) and Leu-2185 (5.38Å), π-σ interaction between the *t*-butyl substituent of ring A with Trp-2239 (3.61Å).
7	Conventional H-bond between the nitro substituent of ring A and Val-2240 (2.66 Å).
10	Alkyl interaction between the isopropyl substituent of ring A with Leu-2185 (4.46 Å), Ile-2356 (4.65 Å) and Ile-2237 (5.39 Å and 5.23 Å), π-alkyl interaction between the isopropyl substituent of ring A with Tyr-2225 (3.78 Å) and Trp-2239 (4.55 Å and 4.26 Å).
13	π-alkyl interaction of Br and Trp-2239 (3.77 Å and 3.90 Å), alkyl interaction of Br and Met-2345 (4.99 Å).
14	π-alkyl interaction between the methyl substituent of ring A with Tyr-2225 (4.34 Å), alkyl interaction between the methyl substituent of ring A with Ile-2356 (4.49 Å) and Ile-2237 (5.34 Å).
15	π-alkyl interaction between the ethyl substituent of ring A and Trp-2239 (5.19Å).
16	Alkyl interaction between the *t*-butyl substituent of ring A with Ile-2356 (4.96 Å) and Leu-2185 (5.15 Å).
17	Conventional H-bond between the nitro substituent of ring A with Val-2240 (2.70 Å).

We can see in Table 11 that some substituents are engaged in short-range interactions with the binding site. They are of the conventional H-bond kind and they should be included with all short-range interactions in the formal model employed for the LMRA analysis. Unhappily we still cannot find a formal way to do it.

Structure-activity results

The beta values (Table 5) indicate that the importance of the variables is $F_{12}(LUMO)^*$ >> $S_8^N(LUMO+2)^*$ > $S_{24}^N(LUMO+2)^*$ > $S_{20}^N(LUMO+2)^*$ > $F_{30}(LUMO+1)^*$. A variable-by-variable (VbV) analysis of Eq. 2 indicates that a high inhibitory percentage is associated with high values for $F_{12}(LUMO)^*$ and $F_{30}(LUMO+1)^*$. The case of the nucleophilic superdelocalizabilities should be analyzed as follows. $S_8^N(LUMO+2)^*$ may have a positive or negative numerical value. If the value of $S_8^N(LUMO+2)^*$ is positive, and because of the negative sign accompanying it in Eq. 2, a high inhibitory percentage is associated with a small value of $S_8^N(LUMO+2)^*$. The contrary must occur if the sign is positive. In the first case a small value of $S_8^N(LUMO+2)^*$ is obtained by shifting upwards the associated eigenvalue and making $(LUMO+2)_8^*$ less reactive. For the second case the analysis leads to the same conclusion. This same reasoning applies to $S_{20}^N(LUMO+2)^*$: a less reactive $(LUMO+2)_{20}^*$ is associated with a high inhibitory percentage. In the case of $S_{24}^N(LUMO+2)^*$ the sign accompanying it in Eq. 2 indicates that a high inhibitory percentage is associated with high values of this variable if its numerical value is positive. If the numerical value of $S_{24}^N(LUMO+2)^*$ is negative, a high inhibitory percentage is associated with a highly negative numerical value for $S_{24}^N(LUMO+2)^*$. Both conditions are associated with a more reactive $(LUMO+2)_{24}^*$. Two important facts are that the variation of the inhibitory percentage is fully orbital-controlled and involves only vacant molecular orbitals. Atom 12 is a carbon one located in ring A. $(LUMO)_{12}^*$ is a π MO (Table 3). A high $F_{12}(LUMO)^*$ value suggests that this atom is interacting with an electron deficient center. Inspecting the docking results (Figs. 5-9) atom 12 seems to participate in π-alkyl and/or π-σ interactions. Atom 30 is the hydrogen bonded to C3. $(LUMO+1)_{30}^*$ is a σ MO (Table 4). A high value of $F_{30}(LUMO+1)^*$ is suggesting that $(LUMO)_{30}^*$ (also a σ MO) and $(LUMO+1)_{30}^*$ are interacting through a carbon H bond with a carbonyl oxygen. This interaction appears in several dockings (see Figs. 5-9). Atom 8 is an oxygen atom in ring B. $(LUMO+2)_8^*$ is a π MO (Table 3). $(LUMO)_8^*$ and $(LUMO+1)_8^*$, both of π nature, do not appear in Eq. 2. It is highly probably that the two highest occupied MOs of atom 8 form part of the

aromatic system of ring B engaged in π-alkyl interactions. Nevertheless, a low value for $S_8^N(LUMO+2)^*$ suggests that this MO seems to be engaged in an unfavorable MO-MO interaction with vacant MOs localized close to it. Atom 20 is a nitrogen atom in ring C. $(LUMO+2)_{20}^*$ is a π MO (Table 3). $(LUMO+1)_{20}^*$ and $(LUMO)_{20}^*$ have also a π nature. A low value for $S_{20}^N(LUMO+2)^*$ can be interpreted like the previous case: an unfavorable interaction with vacant MOs of a moiety. Atom 24 is an oxygen atom in ring D. $(LUMO+2)_{24}^*$ is a σ MO (Table 4). $(LUMO)_{24}^*$ and $(LUMO+1)_{24}^*$ are of lone pair nature. We can expect therefore that atom 24 be engaged in H-bonds (conventional and/or carbon H bonds). The fact that a high value for $(LUMO+2)_{24}^*$ is associated with a high inhibitory percentage suggest that σ electrons are also participating in interactions with a residue (σ-alkyl interactions for example). All these ideas are encompassed in the corresponding two dimensional (2D) pharmacophore shown in Fig. 11.

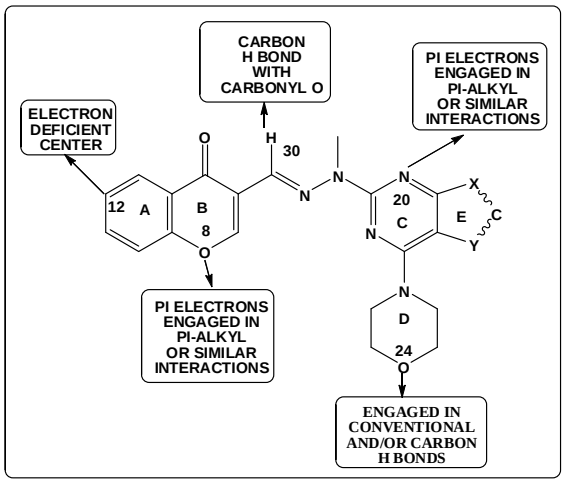

Figure 11. 2D pharmacophore from Eq. 2

What is the exact nature of the relationships between QSAR and docking results? LMRA results show only those reactivity indices whose numerical variation gives an account of the variation of the biological activity studied. Those indices having a constant numerical value do not appear in the final QSAR equations. This seems to be a shortcoming of the formal method but it helps by providing clear atomic targets serving for possible chemical modifications. In this sense the indices appearing in the QSAR equations must be present, in a way or another, in the docking results. Regarding the docking *modus operandi*, it is not a quantum-chemical method. Sometimes very different results are obtained when we allow conformational flexibility to a number of residues forming or being close to the binding site. Sometimes ligands bind to a common site but their common skeleton is located in different forms. Presenting an experimentally measured biological activity of a given number of molecules together with only the crystallized ligand-site structure of one or two molecules can be misleading for some cases. For the moment the wisest approach is to carefully analyze all available information before undertaking a QSAR study.

Selleckchem.com is gratefully acknowledged for allowing the reproduction of Fig. 1.

REFERENCES

[1] VA Polunovskiĭ; PJ Houghton, *mTOR pathway and mTOR inhibitors in cancer therapy*, Humana Press, New York, 2010.
[2] T Weichhart, *mTor: methods and protocols*, Humana Press, New York, 2012.
[3] R Yuge; Y Kitadai; K Shinagawa; M Onoyama; S Tanaka, et al., *Amer. J. Pathol.*, **2015**, 185, 399-408.
[4] N Vajpayee; R Burack; D Wang; RE Hutchison; A Gajra, *Clin. Lymph. Myel. Leuk.*, **2015**, 15, 159-163.

[5] CA Torres; D Garton; W Setlik; M Gershon; D Sulzer, *Drug Alcohol. Dep.*, **2015**, 146, e6.
[6] George P Souroullas; Norman E Sharpless, *Canc. Cell*, **2015**, 27, 3-5.
[7] D Saleiro; LC Platanias, *Trends Immunol.*, **2015**, 36, 21-29.
[8] K Sadowski; K Kotulska-Jóźwiak; S Jóźwiak, *Pharmacol. Rep.*, **2015**, 67, 636-646.
[9] DR Roque; L Yuan; WZ Wysham; C Zhou; VL Bae-Jump, *Gynecol. Oncol.*, **2015**, 137, Supplement 1, 132-133.
[10] KN Pollizzi; JD Powell, *Trends Immunol.*, **2015**, 36, 13-20.
[11] MN Moore, *Environ. Res.*, **2015**, 140, 65-75.
[12] JJ McMahon; W Yu; J Yang; H Feng; M Helm, et al., *Neurobiol. Dis.*, **2015**, 73, 296-306.
[13] S Mabuchi; H Kuroda; R Takahashi; T Sasano, *Gynecol. Oncol.*, **2015**, 137, 173-179.
[14] C-Y Li; X Li; S-F Liu; W-S Qu; W Wang; D-S Tian, *Neurochem. Int.*, **2015**, 83–84, 9-18.
[15] DJ Kwiatkowski; N Wagle, *EBioMedicine*, **2015**, 2, 2-4.
[16] N Houédé; P Pourquier, *Pharmacol. Ther.*, **2015**, 145, 1-18.
[17] T Horng, *Trends Immunol.*, **2015**, 36, 1-2.
[18] H Holdaas; L Potena; F Saliba, *Transpl. Rev.*, **2015**, 29, 93-102.
[19] MY Follo; L Manzoli; A Poli; JA McCubrey; L Cocco, *Adv. Biol. Regul.*, **2015**, 57, 10-16.
[20] F Chiarini; C Evangelisti; JA McCubrey; AM Martelli, *Trends Pharmacol. Sci.*, **2015**, 36, 124-135.
[21] T-C Chen; C-T Wu; C-P Wang; T-L Yang; P-J Lou, et al., *Oral Oncol.*, **2015**, 51, 493-499.
[22] C Cerella; A Gaigneaux; M Dicato; M Diederich, *Canc. Lett.*, **2015**, 356, 251-262.
[23] JA Burket; AD Benson; AH Tang; SI Deutsch, *Progr. Neuro-Psychopharm. Biol. Psych.*, **2015**, 60, 60-65.
[24] V Albert; MN Hall, *Curr. Op. Cell Biol.*, **2015**, 33, 55-66.
[25] F Yang; X Chu; M Yin; X Liu; H Yuan, et al., *Behav. Brain Res.*, **2014**, 264, 82-90.
[26] K Xu; P Liu; W Wei, *Biochem. Bioph. Acta. Rev. Canc.*, **2014**, 1846, 638-654.
[27] JR Westin, *Clin. Lymph. Myel. Leuk.*, **2014**, 14, 335-342.
[28] K Watson; K Baar, *Sem. Cell. Dev. Biol.*, **2014**, 36, 130-139.
[29] AR Tee, *Sem. Cell. Dev. Biol.*, **2014**, 36, 66-67.
[30] G Silva; M Tsujita; E Santos; J Beltran; P Borelli, *Exp. Hematol.*, **2014**, 42, S60.
[31] J Robert, *Bull. Canc.*, **2014**, 101, 775.
[32] J Polivka Jr; F Janku, *Pharmacol. Ther.*, **2014**, 142, 164-175.
[33] M Perluigi; G Pupo; A Tramutola; C Cini; R Coccia, et al., *Biochem. Bioph. Acta Mol. Bas. Dis.*, **2014**, 1842, 1144-1153.
[34] H Northrup, *Lancet Oncol.*, **2014**, 15, 1418-1419.
[35] Jonathan O Lipton; M Sahin, *Neuron*, **2014**, 84, 275-291.
[36] SC Land; CL Scott; D Walker, *Sem. Cell. Dev. Biol.*, **2014**, 36, 68-78.
[37] K Inoki, *Sem. Nephrol.*, **2014**, 34, 2-8.
[38] K Huang; DC Fingar, *Sem. Cell. Dev. Biol.*, **2014**, 36, 79-90.
[39] Y Hu; J Liu; Y-F Wu; J Lou; Y-Y Mao, et al., *Microb. Infect.*, **2014**, 16, 727-734.
[40] A Handra-Luca, *Human Pathol.*, **2014**, 45, 895-897.
[41] M Haissaguerre; N Saucisse; D Cota, *Mol. Cell. Endocrinol.*, **2014**, 397, 67-77.
[42] V Gopalan; RA Smith; AK-y Lam, *Human Pathol.*, **2014**, 45, 897.
[43] BD Fonseca; EM Smith; N Yelle; T Alain; M Bushell; A Pause, *Sem. Cell. Dev. Biol.*, **2014**, 36, 102-112.
[44] D Baretić; RL Williams, *Sem. Cell. Dev. Biol.*, **2014**, 36, 91-101.
[45] HM Abelaira; GZ Réus; MV Neotti; J Quevedo, *Life Sci.*, **2014**, 101, 10-14.
[46] H Zeng; H Chi, *Curr. Op. Immunol.*, **2013**, 25, 347-355.
[47] G Panasyuk; C Patitucci; C Espeillac; M Pende, *Ann. d'Endocrinol.*, **2013**, 74, 121-122.
[48] PN Morehead; L Kong; J Kang; MM Solis; DK Nakayama; Z Wang, *J. Amer. Coll. Surg.*, **2013**, 217, S159.
[49] X-F Meng; J-T Yu; J-H Song; S Chi; L Tan, *J. Neurol. Sci.*, **2013**, 332, 4-15.
[50] K Maiese; ZZ Chong; YC Shang; S Wang, *Trends Mol. Med.*, **2013**, 19, 51-60.
[51] Dudley W Lamming; David M Sabatini, *Cell Met.*, **2013**, 18, 465-469.
[52] JL Jewell; K-L Guan, *Trends Biochem. Sci.*, **2013**, 38, 233-242.
[53] DA Foster, *Trends Endocrinol. Metab.*, **2013**, 24, 272-278.
[54] M Cornu; V Albert; MN Hall, *Curr. Op. Genet. Dev.*, **2013**, 23, 53-62.
[55] AF Abdel-Magid, *ACS Med. Chem. Lett.*, **2013**, 4, 321-322.
[56] F Zagouri; TN Sergentanis; D Chrysikos; M Filipits; R Bartsch, *Gynecol. Oncol.*, **2012**, 127, 662-672.
[57] X Xu; L Ye; K Araki; R Ahmed, *Sem. Immunol.*, **2012**, 24, 429-435.
[58] SM Smith, *Best Pract. Res. Clin. Haematol.*, **2012**, 25, 175-183.
[59] W Zhu; C Chen; C Sun; S Xu; C Wu, et al., *Eur. J. Med. Chem.*, **2015**, 93, 64-73.

[60]Q Tian; U Hoffmann; T Humphries; Z Cheng; P Hidber, et al., *Organic Process Research & Development*, **2015**, 19, 416-426.
[61]Y-H Cui; J Chen; T Xu; H-L Tian, *Comput. Biol. Chem.*, **2015**, 54, 57-65.
[62]W Zhu; C Sun; S Xu; C Wu; J Wu, et al., *Biorg. Med. Chem.*, **2014**, 22, 6746-6754.
[63]T Saurat; F Buron; N Rodrigues; M-L de Tauzia; L Colliandre, et al., *J. Med. Chem.*, **2014**, 57, 613-631.
[64]C Salomé; V Narbonne; N Ribeiro; F Thuaud; M Serova, et al., *Eur. J. Med. Chem.*, **2014**, 74, 41-49.
[65]GL Reddy; SK Guru; M Srinivas; AS Pathania; P Mahajan, et al., *Eur. J. Med. Chem.*, **2014**, 80, 201-208.
[66]C Loos; T Syrovets; A Musyanovych; V Mailänder; K Landfester; T Simmet, *Biomater.*, **2014**, 35, 1944-1953.
[67]S Lin; F Han; P Liu; J Tao; X Zhong, et al., *Biorg. Med. Chem. Lett.*, **2014**, 24, 790-793.
[68]F Han; S Lin; P Liu; J Tao; C Yi; H Xu, *Biorg. Med. Chem. Lett.*, **2014**, 24, 4538-4541.
[69]B Gobin; S Battaglia; R Lanel; J Chesneau; J Amiaud, et al., *Canc. Lett.*, **2014**, 344, 291-298.
[70]X Feng; L Li; H Jiang; K Jiang; Y Jin; J Zheng, *Biochem. Biophys. Res. Comm.*, **2014**, 444, 376-381.
[71]W Yang; M Shu; Y Wang; R Wang; Y Hu, et al., *J. Mol. Struct.*, **2013**, 1054–1055, 107-116.
[72]ME Welker; G Kulik, *Biorg. Med. Chem.*, **2013**, 21, 4063-4091.
[73]W Lee; DF Ortwine; P Bergeron; K Lau; L Lin, et al., *Biorg. Med. Chem. Lett.*, **2013**, 23, 5097-5104.
[74]H Cheng; C Li; S Bailey; SM Baxi; L Goulet, et al., *ACS Med. Chem. Lett.*, **2013**, 4, 91-97.
[75]H Cheng; JE Hoffman; PT Le; M Pairish; R Kania, et al., *Biorg. Med. Chem. Lett.*, **2013**, 23, 2787-2792.
[76]S Xu; T Tran; T Tsuji; L Sapinoso; KE Fultz, et al., *Eur. J. Canc.*, **2012**, 48, Supplement 6, 103.
[77]J Tabernero; R Dienstmann; T Macarulla; C Saura; G Argiles, et al., *Eur. J. Canc.*, **2012**, 48, Supplement 6, 3.
[78]A Poulsen; M Williams; HM Nagaraj; AD William; H Wang, et al., *Biorg. Med. Chem. Lett.*, **2012**, 22, 1009-1013.
[79]EA Peterson; AA Boezio; PS Andrews; CM Boezio; TL Bush, et al., *Biorg. Med. Chem. Lett.*, **2012**, 22, 4967-4974.
[80]PT Le; H Cheng; S Ninkovic; M Plewe; X Huang, et al., *Biorg. Med. Chem. Lett.*, **2012**, 22, 6774.
[81]PT Le; H Cheng; S Ninkovic; M Plewe; X Huang, et al., *Biorg. Med. Chem. Lett.*, **2012**, 22, 5098-5103.
[82]MRV Finlay; D Buttar; SE Critchlow; AP Dishington; SM Fillery, et al., *Biorg. Med. Chem. Lett.*, **2012**, 22, 4163-4168.
[83]MM Stec; KL Andrews; SK Booker; S Caenepeel; DJ Freeman, et al., *J. Med. Chem.*, **2011**, 54, 5174-5184.
[84]EA Peterson; PS Andrews; X Be; AA Boezio; TL Bush, et al., *Biorg. Med. Chem. Lett.*, **2011**, 21, 2064-2070.
[85]Q Liu; J Wang; SA Kang; CC Thoreen; W Hur, et al., *Biorg. Med. Chem. Lett.*, **2011**, 21, 4036-4040.
[86]Q Liu; J Wang; SA Kang; CC Thoreen; W Hur, et al., *J. Med. Chem.*, **2011**, 54, 1473-1480.
[87]KKC Liu; X Huang; S Bagrodia; JH Chen; S Greasley, et al., *Biorg. Med. Chem. Lett.*, **2011**, 21, 1270-1274.
[88]ND D'Angelo; T-S Kim; K Andrews; SK Booker; S Caenepeel, et al., *J. Med. Chem.*, **2011**, 54, 1789-1811.
[89]N Zhang; S Ayral-Kaloustian; JT Anderson; T Nguyen; S Das, et al., *Biorg. Med. Chem. Lett.*, **2010**, 20, 3526-3529.
[90]A Zask; JC Verheijen; DJ Richard; J Kaplan; K Curran, et al., *Biorg. Med. Chem. Lett.*, **2010**, 20, 2644-2647.
[91]JC Verheijen; K Yu; L Toral-Barza; I Hollander; A Zask, *Biorg. Med. Chem. Lett.*, **2010**, 20, 375-379.
[92]JC Verheijen; DJ Richard; K Curran; J Kaplan; K Yu; A Zask, *Biorg. Med. Chem. Lett.*, **2010**, 20, 2648-2653.
[93]AM Venkatesan; CM Dehnhardt; Z Chen; ED Santos; O Dos Santos, et al., *Biorg. Med. Chem. Lett.*, **2010**, 20, 653-656.
[94]H-R Tsou; G MacEwan; G Birnberg; N Zhang; N Brooijmans, et al., *Biorg. Med. Chem. Lett.*, **2010**, 20, 2259-2263.
[95]H-R Tsou; G MacEwan; G Birnberg; G Grosu; MG Bursavich, et al., *Biorg. Med. Chem. Lett.*, **2010**, 20, 2321-2325.
[96]DP Sutherlin; D Sampath; M Berry; G Castanedo; Z Chang, et al., *J. Med. Chem.*, **2010**, 53, 1086-1097.
[97]Q Liu; JW Chang; J Wang; SA Kang; CC Thoreen, et al., *J. Med. Chem.*, **2010**, 53, 7146-7155.
[98]KKC Liu; S Bagrodia; S Bailey; H Cheng; H Chen, et al., *Biorg. Med. Chem. Lett.*, **2010**, 20, 6096-6099.
[99]KJ Curran; JC Verheijen; J Kaplan; DJ Richard; L Toral-Barza, et al., *Biorg. Med. Chem. Lett.*, **2010**, 20, 1440-1444.
[100]S Ayral-Kaloustian; J Gu; J Lucas; M Cinque; C Gaydos, et al., *J. Med. Chem.*, **2010**, 53, 452-459.
[101]KA Menear; S Gomez; K Malagu; C Bailey; K Blackburn, et al., *Biorg. Med. Chem. Lett.*, **2009**, 19, 5898-5901.
[102]K Malagu; H Duggan; K Menear; M Hummersone; S Gomez, et al., *Biorg. Med. Chem. Lett.*, **2009**, 19, 5950-5953.
[103]Q Liu; C Thoreen; J Wang; D Sabatini; NS Gray, *Drug Disc. Tod. Ther. Strat.*, **2009**, 6, 47-55.
[104]V Deore; N Yewalkar; D Bhatia; N Desai; RD Gupte, et al., *Biorg. Med. Chem. Lett.*, **2009**, 19, 2949-2952.

[105]MV Lohar; R Mundada; M Bhonde; A Padgaonkar; V Deore, et al., *Biorg. Med. Chem. Lett.*, **2008**, 18, 3603-3606.
[106]YC Martin, *Quantitative drug design: a critical introduction*, M. Dekker, New York, **1978**.
[107]D Agin; L Hersh; D Holtzman, *Proc. Natl. Acad. Sci. (USA)*, **1965**, 53, 952-958.
[108]F Peradejordi; AN Martin; A Cammarata, *J. Pharm. Sci.*, **1971**, 60, 576-582.
[109]F Tomas; JM Aulló, *J. Pharm. Sci.*, **1979**, 68, 772-776.
[110]JS Gómez-Jeria, *Int. J. Quant. Chem.*, **1983**, 23, 1969-1972.
[111]JS Gómez-Jeria, "Modeling the Drug-Receptor Interaction in Quantum Pharmacology," in *Molecules in Physics, Chemistry, and Biology*, J. Maruani Ed., vol. 4, pp. 215-231, Springer Netherlands, **1989**.
[112]JS Gómez-Jeria; M Ojeda-Vergara, *J. Chil. Chem. Soc.*, **2003**, 48, 119-124.
[113]K Fukui; H Fujimoto, *Frontier orbitals and reaction paths: selected papers of Kenichi Fukui*, World Scientific, Singapore; River Edge, N.J., **1997**.
[114]JS Gómez-Jeria, *Canad. Chem. Trans.*, **2013**, 1, 25-55.
[115]JS Gómez-Jeria; DR Morales-Lagos, *J. Pharm. Sci.*, **1984**, 73, 1725-1728.
[116]JS Gómez-Jeria; D Morales-Lagos; BK Cassels; JC Saavedra-Aguilar, *Quant. Struct.-Relat.*, **1986**, 5, 153-157.
[117]JS Gómez-Jeria; M Ojeda-Vergara; C Donoso-Espinoza, *Mol. Engn.*, **1995**, 5, 391-401.
[118]JS Gómez-Jeria; L Lagos-Arancibia; E Sobarzo-Sánchez, *Bol. Soc. Chil. Quím.*, **2003**, 48, 61-66.
[119]JS Gómez-Jeria, *J. Chil. Chem. Soc.*, **2010**, 55, 381-384.
[120]JS Gómez-Jeria; A Robles-Navarro, *Res. J. Pharmac. Biol. Chem. Sci.*, **2015**, 6, in press.
[121]JS Gómez-Jeria; A Robles-Navarro, *Res. J. Pharmac. Biol. Chem. Sci.*, **2015**, 6, 1811-1841.
[122]JS Gómez-Jeria; A Robles-Navarro, *Der Pharma Chem.*, **2015**, 7, 243-269.
[123]R Solís-Gutiérrez; JS Gómez-Jeria, *Res. J. Pharmac. Biol. Chem. Sci.*, **2014**, 5, 1401-1416.
[124]JS Gómez-Jeria; J Molina-Hidalgo, *J. Comput. Methods Drug Des.*, **2014**, 4, 1-9.
[125]JS Gómez-Jeria, *SOP Trans. Phys. Chem.*, **2014**, 1, 10-28.
[126]JS Gómez-Jeria, *Der Pharm. Lett.*, **2014**, 6., 95-104.
[127]T Bruna-Larenas; JS Gómez-Jeria, *Int. J. Med. Chem.*, **2012**, 2012 Article ID 682495, 1-16.
[128]F Salgado-Valdés; JS Gómez-Jeria, *J. Quant. Chem.*, **2014**, 2014 Article ID 431432, 1-15.
[129]MS Leal; A Robles-Navarro; JS Gómez-Jeria, *Der Pharm. Lett.*, **2015**, 7, 54-66.
[130]JS Gómez-Jeria; A Robles-Navarro, *Res. J. Pharmac. Biol. Chem. Sci.*, **2015**, 6, 755-783.
[131]JS Gómez-Jeria; A Robles-Navarro, *Res. J. Pharmac. Biol. Chem. Sci.*, **2015**, 6, 1337-1351.
[132]DI Pino-Ramírez; JS Gómez-Jeria, *Amer. Chem. Sci. J.*, **2014**, 4, 554-575.
[133]D Muñoz-Gacitúa; JS Gómez-Jeria, *J. Comput. Methods Drug Des.*, **2014**, 4, 48-63.
[134]D Muñoz-Gacitúa; JS Gómez-Jeria, *J. Comput. Methods Drug Des.*, **2014**, 4, 33-47.
[135]JS Gómez-Jeria; J Valdebenito-Gamboa, *Der Pharma Chem.*, **2014**, 6, 383-406.
[136]JS Gómez-Jeria, *Res. J. Pharmac. Biol. Chem. Sci.*, **2014**, 5, 780-792.
[137]JS Gómez-Jeria, *J. Comput. Methods Drug Des.*, **2014**, 4, 38-47.
[138]JS Gómez-Jeria, *Res. J. Pharmac. Biol. Chem. Sci.*, **2014**, 5, 424-436.
[139]JS Gómez-Jeria, *J. Comput. Methods Drug Des.*, **2014**, 4, 32-44.
[140]JS Gómez-Jeria, *Res. J. Pharmac. Biol. Chem. Sci.*, **2014**, 5, 2124-2142.
[141]JS Gómez-Jeria, *Der Pharma Chem.*, **2014**, 6, 64-77.
[142]JS Gómez-Jeria, *Brit. Microbiol. Res. J.*, **2014**, 4, 968-987.
[143]JS Gómez-Jeria, *Int. Res. J. Pure App. Chem.*, **2014**, 4, 270-291.
[144]F Gatica-Díaz; JS Gómez-Jeria, *J. Comput. Methods Drug Des.*, **2014**, 4, 79-120.
[145]I Reyes-Díaz; JS Gómez-Jeria, *J. Comput. Methods Drug Des.*, **2013**, 3, 11-21.
[146]A Paz de la Vega; DA Alarcón; JS Gómez-Jeria, *J. Chil. Chem. Soc.*, **2013**, 58, 1842-1851.
[147]JS Gómez-Jeria; M Flores-Catalán, *Canad. Chem. Trans.*, **2013**, 1, 215-237.
[148]DA Alarcón; F Gatica-Díaz; JS Gómez-Jeria, *J. Chil. Chem. Soc.*, **2013**, 58, 1651-1659.
[149]C Barahona-Urbina; S Nuñez-Gonzalez; JS Gómez-Jeria, *J. Chil. Chem. Soc.*, **2012**, 57, 1497-1503.
[150]MJ Frisch; GW Trucks; HB Schlegel; GE Scuseria; MA Robb, et al., G03 Rev. E.01, Gaussian, Pittsburgh, PA, USA, **2007**.
[151]JS Gómez-Jeria, *J. Chil. Chem. Soc.*, **2009**, 54, 482-485.
[152]JS Gómez-Jeria, D-Cent-QSAR: A program to generate Local Atomic Reactivity Indices from Gaussian 03 log files. 1.0, Santiago, Chile, **2014**.
[153]Statsoft, Statistica 8.0, 2300 East 14 th St. Tulsa, OK 74104, USA, **1984-2007**.
[154]O Trott; AJ Olson, *J. Comput. Chem.*, **2010**, 31, 455-461.

[155]Accelrys Software Inc., Discovery Studio Visualizer 4.1, Accelrys Software Inc., San Diego, CA, USA, 2013.
[156]Z Latajka; S Scheiner, *Int. J. Quant. Chem.*, **1986**, 29, 285-292.
[157]GR Desiraju; T Steiner, *The weak hydrogen bond: in structural chemistry and biology*, Oxford University Press, Oxford; New York, **1999**.
[158]JS Gómez-Jeria; A Robles-Navarro, *Der Pharma Chem.*, **2015**, 7, 230-241.
[159]JS Gómez-Jeria; A Robles-Navarro, *J. Comput. Methods Drug Des.*, **2015**, 5, 45-47.